

The Incorporation of Extracellular Vesicles from Mesenchymal Stromal Cells Into CD34⁺ Cells Increases Their Clonogenic Capacity and Bone Marrow Lodging Ability

SILVIA PRECIADO,^{a,b,c,d} SANDRA MUNTIÓN ^{a,b,d}, LUIS A. CORCHETE,^a TERESA L. RAMOS,^{d,e} ANA G. DE LA TORRE,^{a,f} LIKA OSUGUI,^a ANA RICO,^{a,b} NATALIA ESPINOSA-LARA,^{a,b} IRENE GASTACA,^g MARÍA DÍEZ-CAMPELO,^{a,c,d} CONSUELO DEL CAÑIZO,^{a,b,c,d,f} FERMÍN SÁNCHEZ-GUIJO^{a,b,c,d,f}

Key Words. Engraftment • Extracellular vesicles • Stem cell transplantation • Mesenchymal stromal cells • Hematopoietic stem cells

^aServicio de Hematología, IBSAL-Hospital Universitario de Salamanca, Salamanca, Spain; ^bCentro en Red de Medicina Regenerativa y Terapia Celular de Castilla y León, Salamanca, Spain; ^cDepartment of Medicine, Universidad de Salamanca, Salamanca, Spain; ^dRETIC TerCel, ISCIII, Salamanca, Spain; ^eLaboratorio de Terapia Celular, Instituto de Biomedicina de Sevilla (IBIS), UGC-Hematología, Hospital Universitario Virgen del Rocío/CSIC/CIBERONC, Sevilla, Spain; ^fCentro de Investigación del Cáncer, Universidad de Salamanca, Salamanca, Spain; ^gServicio de Ginecología, Hospital Universitario de Salamanca, Salamanca, Spain

Correspondence: Sandra Muntión, Ph.D., Servicio de Hematología, IBSAL-Hospital Universitario de Salamanca, Paseo San Vicente 58-182, Salamanca 37007, Spain. Telephone: 923 291100; e-mail: smuntion@usal.es

Received November 15, 2018; accepted for publication April 20, 2019; first published online in June 11, 2019.

<http://dx.doi.org/10.1002/stem.3032>

This is an open access article under the terms of the Creative Commons Attribution-NonCommercial-NoDerivs License, which permits use and distribution in any medium, provided the original work is properly cited, the use is non-commercial and no modifications or adaptations are made.

ABSTRACT

Mesenchymal stromal cells (MSC) may exert their functions by the release of extracellular vesicles (EV). Our aim was to analyze changes induced in CD34⁺ cells after the incorporation of MSC-EV. MSC-EV were characterized by flow cytometry (FC), Western blot, electron microscopy, and nanoparticle tracking analysis. EV incorporation into CD34⁺ cells was confirmed by FC and confocal microscopy, and then reverse transcription polymerase chain reaction and arrays were performed in modified CD34⁺ cells. Apoptosis and cell cycle were also evaluated by FC, phosphorylation of signal activator of transcription 5 (STAT5) by WES Simple, and clonal growth by clonogenic assays. Human engraftment was analyzed 4 weeks after CD34⁺ cell transplantation in nonobese diabetic/severe combined immunodeficient mice. Our results showed that MSC-EV incorporation induced a downregulation of proapoptotic genes, an overexpression of genes involved in colony formation, and an activation of the Janus kinase (JAK)-STAT pathway in CD34⁺ cells. A significant decrease in apoptosis and an increased CD44 expression were confirmed by FC, and increased levels of phospho-STAT5 were confirmed by WES Simple in CD34⁺ cells with MSC-EV. In addition, these cells displayed a higher colony-forming unit granulocyte/macrophage clonogenic potential. Finally, the *in vivo* bone marrow lodging ability of human CD34⁺ cells with MSC-EV was significantly increased in the injected femurs. In summary, the incorporation of MSC-EV induces genomic and functional changes in CD34⁺ cells, increasing their clonogenic capacity and their bone marrow lodging ability. *STEM CELLS* 2019;37:1357–1368

SIGNIFICANCE STATEMENT

In the current study, the authors validate for the first time that preincubating human CD34⁺ cells with extracellular vesicles derived from human mesenchymal stromal cells not only modifies the gene expression of the recipient cells (inducing a downregulation of proapoptotic genes and overexpression of genes involved in colony formation and JAK-STAT pathway) but also significantly increases their *in vitro* clonogenic ability and, most importantly, increases their 4-week bone marrow lodging ability *in vivo* in a standard xenotransplantation model. This strategy could potentially be exploited to increase the hematopoietic engraftment in the clinical setting.

INTRODUCTION

Graft failure or poor engraftment and their consequences are important complications after allogeneic stem cell transplantation (allo-SCT). Such complications can be caused by an insufficient number of transplanted cells, by the presence of antibodies, or by a defective stroma [1–3].

It should be noted that bone marrow (BM) stroma remains of host origin after allo-SCT and can be damaged because of a number of factors,

including chemotherapy, infections or their treatments, graft-versus-host disease, or high-dose radiotherapy [4, 5].

Mesenchymal stromal cells (MSC) play an important role in the regulation of most cells of the BM microenvironment [6–8]. From a therapeutic perspective, the administration of MSC has been shown to increase the engraftment ability and the hematopoietic function in preclinical models of xenotransplantation [9–13]. In addition, it has been shown that the

administration of MSC from third-party donors can also potentially increase the engraftment and improve post-transplant cytopenias [14, 15].

It has been recently demonstrated that some of the beneficial effects of MSC can be exerted through the release of extracellular vesicles (EV) [16, 17]. Although there are several types of EV depending on their size and origin (e.g., exosomes, microvesicles, and apoptotic bodies), all EV are small-size membrane-derived particles that selectively carry some mRNA, microRNA, lipids, and proteins that can be incorporated into recipient cells and modify their function [18–21].

Several groups have shown that MSC-EV participate in the communication between microenvironment and CD34⁺ cells [18, 22, 23]. Recent studies have demonstrated that EV released by MSC could have similar effects to those of MSC [24–26].

In the current work, we wanted to evaluate multiparametrically the changes induced in CD34⁺ cells after the incorporation of MSC-derived EV. Moreover, we have assessed if this incorporation has functional implications, evaluating their clonogenic ability in vitro and the in vivo engraftment in a xenotransplantation model.

MATERIALS AND METHODS

MSC Isolation and Expansion

BM-MSC were isolated from 48 healthy donors (29 males and 19 females) with a median age of 40 years (range 18–83 years), after written informed consent was obtained. All experimental procedures were approved by local Ethics Committee (code 70/07/2015).

BM mononuclear cells (BM-MNC) were isolated by density-gradient centrifugation (Ficoll-Paque, density: 1.077 g/ml, GE Healthcare-BioSciences). Cells were seeded at a density of 1×10^6 cells per centimeter square and expanded as previously described at 37°C and 5% of CO₂ in a humidified atmosphere [27, 28] in Dulbecco's modified Eagle's medium-low glucose (Gibco, Life-Technologies) with 10% fetal bovine serum (Gibco, Life Technologies) and 1% penicillin/streptomycin. After third passage, MSC were assessed according to the criteria proposed by the International Society for Cellular Therapy (ISCT) [29].

CD34⁺ Cell Isolation

CD34⁺ cells were isolated from residual material from leukapheresis products of 33 healthy donors (23 males and 10 females) with a median age of 47 years (range 20–71 years) used in our Transplant Program. A small aliquot (1 ml) of fresh leukapheresis products from healthy volunteer donors in our allogeneic stem cell transplant program was used for the study. All donors had been prior evaluated in our pretransplant clinic, and informed consent was obtained to obtain an aliquot for research purposes in case the CD34⁺ cell counts obtained exceeded the required maximum amount for a standard sibling allo-SCT according to institutional standard operational procedures. CD34⁺ cells were purified by immunomagnetic sorting in an AutoMACS (MiltenyiBiotec GmbH) after labeling with the human CD34 MicroBead Kit (MiltenyiBiotec). Purity and viability of cells was confirmed by flow cytometry (FC). The mobilization regimen for the donors was exclusively filgrastim at 5 µg/kg/12 hours during 4 days.

Only for xenotransplantation experiments (see below), CD34⁺ cells were isolated from umbilical cord blood (UCB),

based on the higher in vivo engraftment ability compared with adult CD34⁺ cells [30]. Ten fresh UCB units were either purchased from the Barcelona Blood and Tissue Bank and CHEMCYL or kindly provided by the Obstetrics Department of Hospital Universitario de Salamanca following standard procedures, after proper informed consent was obtained from the corresponding mothers. MNCs were isolated by Ficoll-Paque density gradient centrifugation, and then CD34⁺ cells were isolated following the same protocol used for leukapheresis-derived cells. Nevertheless, to confirm that some of the observed results were also induced in cord-blood cells, some experiments were additionally performed and are included in Supporting Information Figure S2.

EV Isolation and Characterization

To avoid collecting EV from fetal calf serum, the latter was removed from the culture medium for 12 hours. Then, the supernatant was collected and centrifuged at 3,000g for 20 minutes and then at 10,000g for 30 minutes. Supernatants were then ultracentrifuged at 100,000g for 70 minutes at 4°C using a Beckman Coulter OptimaL-90K ultracentrifuge (Fullerton, CA) [31]. Then, EV were characterized by:

- Nanoparticle tracking analysis (NTA): EV size distribution and the amount of particles per millimeter were quantified using a NanoSight LM10 instrument (Nanosight Ltd., UK) with the NTA2.0 software.
- Transmission electron microscopy (TEM): The EV containing pellet was fixed in 2% paraformaldehyde and 1% glutaraldehyde and processed as described in Supporting Information Methods section. Samples were examined under a TEM (FEITecni G2 Spirit Biotwin) using a digital camera (Morada, Soft Imaging System, Olympus) [32].
- Flow cytometry: For immunophenotypic characterization, EV were incubated with monoclonal antibodies (see Supporting Information Methods section for details). Samples were acquired on a FACSCanto II flow cytometer (BD Biosciences, San Jose, CA) using the FACSDiva 6.1 software (BD Biosciences). The cytometer was previously calibrated and compensated [33]. A mixture of fluorescent beads based on 1 µm monodisperse polystyrene (Sigma-Aldrich) and PerfectCount Microspheres (Cytognos, Salamanca, Spain) of 6–6.4 µm in size was used as a size marker. A total of 10^5 events were acquired. Data were analyzed with the Infinicyt software (Cytognos, Salamanca).
- Western blot: EV were lysed in $\times 1$ RIPA lysis buffer with Phenylmethylsulfonyl fluoride, protease inhibitor cocktail, and sodium orthovanadate. Protein samples were loaded on a 12% SDS-polyacrylamide gel electrophoresis gel and transferred to a poly(vinylidene fluoride) membrane, which was incubated with primary antibody followed by the corresponding horseradish peroxidase conjugated secondary antibody (Supporting Information data). The chemiluminescence was detected using Clarity Western ECL Substrate (BioRad).

Incorporation of EV into CD34⁺ Cells

To allow the incorporation of MSC-EV into human CD34⁺ cells, 1×10^5 CD34⁺ cells were cocultured with MSC-EV for 24 Roswell Park Memorial Institute Medium (RPMI) as it was described before [23]. For each coculture, around 30 µg of protein from MSC-derived EV was used. The same amount of CD34⁺ cells without EV was used as control.

To allow their tracking before coculture, EV were stained with Vybrant Dil cell labeling solution (Life Technology), following manufacturer's instructions [23, 34]. As a control, an ultracentrifugation tube was included containing only phosphate-buffered saline and Vybrant Dil. Then, the incorporation was measured both by FC and confocal microscopy. For the former, cells from 13 samples were stained and acquired in a FACSCalibur flow cytometer and analyzed with Flow JO (Oregon). For immunofluorescence, CD34⁺ cells were processed as indicated in Supporting Information. Cellular nuclei were stained with 4',6-diamidino-2-phenylindole. Cells were viewed with a TCS SP5 Confocal Laser Scanning Microscope (Leica Microsystems GmbH, Wetzlar) with the LAS AF acquisition program (version 2.6.0.7266).

Reverse Transcription Polymerase Chain Reaction of Stromal-Cell-Derived Factor-1 and Collagen Type I Alpha I

Total RNA was extracted from 10 pairs of CD34⁺ cells. cDNA was prepared by reverse transcription using the High Capacity cDNA Reverse Transcription Kit (Applied Biosystems), and the converted cDNA was analyzed for stromal-cell-derived factor-1 (*SDF-1*) and Collagen type I Alpha I (*COL1A1*). Glyceraldehyde-3-phosphate dehydrogenase was used as a control. Genes were quantified using TaqMan Gene Expression Assays and the Step One Plus Real-Time PCR System (Applied Biosystems). Relative quantification was calculated from the $2^{-\Delta C_t}$ values where: $\Delta C_t = C_t^{\text{Gene}} - C_t^{\text{Control}}$.

Gene Chip Human Gene ST Arrays

Total RNA was isolated and purified from five pairs of CD34⁺ cells cocultured for 24 hours using RNeasy Mini Kit (Qiagen, Hilden, Germany), according to manufacturer's instructions. RNA integrity was assessed using Agilent 2100 Bioanalyzer. Labeling and hybridizations were performed according to protocols from Affymetrix in a Human Gene 2.0 ST Array. Washing and scanning were performed using GeneChip System of Affymetrix (GeneChip Hybridization Oven 645, GeneChip Fluidics Station 450 and GeneChip Scanner 7G). The analysis is further detailed in Supporting Information. Genes with a *q*-value <0.05 were considered to be significantly expressed. The functional and pathway analysis was carried out in the Webgestalt application [35]. The Gene Expression Omnibus entry for each sample includes the raw data (code #GSE120803) and is located at the following website link: <https://www.ncbi.nlm.nih.gov/geo/query/acc.cgi?token=exozqmwofdqblmj&acc=GSE120803>

Apoptosis and Caspase Activity Assays

After 24 and 48 hours of coculture, CD34⁺ cells were stained with Annexin V, 7-amino-actinomycin (7-AAD) using the BD Pharmigen PE Annexin V Apoptosis Detection Kit I (BD Biosciences). Cells were also labeled with fluorescein isothiocyanate-conjugated CD34. Samples were acquired on a FACS Calibur device. At least 5×10^4 events were recorded. Data were analyzed using Infinicyt. Cells were considered to be in an early apoptotic state, late apoptosis, or dead if they were Annexin V⁻/7-AAD⁻, Annexin V⁺/7-AAD⁺, or Annexin V⁻/7-AAD⁺, respectively, as previously reported [27] (Supporting Information Fig. S3A). Caspase 3/7 and caspase 9 activity was measured after 24 hours of coculture using the Caspase-Glo 3/7 Assay Systems kit and the Caspase-Glo 9 Assay Systems kit (Promega). Ten samples were used to perform these experiments.

Cell Cycle Analysis

Ten samples of CD34⁺ cells were cocultured for 24 hours and stained with propidium iodide using the kit BD Cycletest Plus DNA Reagent Kit (Beckton Dickinson), according to manufacturer's instructions. Samples were acquired in a FACS Calibur flow cytometer and analyzed using ModFit LT V5.0.9 (Verity Software; Supporting Information Fig. S3B).

Flow Cytometric Analysis of Proteins Involved in Hematopoiesis

Ten samples of CD34⁺ cells were incubated with the corresponding monoclonal antibodies (see Supporting Information). Samples were acquired on a FACS Calibur flow cytometer using Cellquest Pro software. Data were analyzed using the Infinicyt software. Data were represented as mean fluorescence intensity (Supporting Information Fig. S4).

Capillary Electrophoresis Immunoassay

Whole-cell lysates were obtained from two samples of CD34⁺ cells with or without incorporation of MSC-EV. Capillary Electrophoresis Immunoassay or Simple Western analyses were performed using the WES machine (ProteinSimple, Santa Clara, CA), according to the manufacturer's protocols [36]. The data were analyzed with inbuilt Compass software (ProteinSimple). Further details are provided in Supporting Information. For the assay, we used primary antibodies Calnexin, signal activator of transcription 5 (STAT5), and p-STAT5 (see also Supporting Information).

Clonogenic Assays

CD34⁺ cells from 10 samples were incubated in different conditions for 24 hours. Then, cells were recovered, and 1,500 cells were seeded into methylcellulose MACS Media Stem MACS HSC-CFU complete without Epo human (Miltenyi Biotec, Germany) to quantify progenitor cell colony-forming unit granulocyte/macrophage (CFU-GM), according to the manufacturer's instructions. After 14 days at 37°C in a fully humidified atmosphere of 5% CO₂, CFU-GM was scored using an inverted microscope.

Analysis of Human Hematopoietic Engraftment in Mice

For in vivo studies, 6-week-old nonobese diabetic/severe combined immunodeficient (NOD/SCID; NOD.CB17-Prkdcscid/NcrCrl) mice were purchased from Charles River Laboratories (Barcelona, Spain) and maintained in the animal care facility of the University of Salamanca. All procedures followed the Spanish and European Union guidelines (RD 1201/05 and 86/609/CEE) and were approved by the Bioethics Committee of the University of Salamanca (reg. 201100007924).

The murine transplant model was established as previously reported with minor modifications [9]. Thirty female mice were used (10 per experimental group). Six hours before transplantation, mice were irradiated with 350 cGy total body irradiation using a cesium source (Gammacell-200, Nordion International). Animals were anesthetized with a mixture of ketamine (90 mg/kg; Imalgene 500) and xylazine (10 mg/kg; Rompun 2%, KVP Pharma). Two experimental groups were established: (1) 2×10^5 UCB CD34⁺ cells and (2) 2×10^5 UCB CD34⁺ cells previously cocultured with MSC-EV. For each coculture, around 60 µg of protein from MSC-derived EV was used. Cocultures were incubated for 24 hours in a volume of 500 µl RPMI per well. Then 1×10^5 cells were administered via intraperitoneally,

through the knee. Four weeks after transplantation, mice were sacrificed and the hematopoietic engraftment was evaluated by FC in the injected femur (right), contralateral femur (left), and spleen [37]. All cell suspensions were collected and red blood cells were lysated. Samples were stained with monoclonal antibodies (specified in Supporting Information). Data analysis is detailed in Supporting Information.

Statistical Analysis

Values were summarized as median and range. The nonparametric Wilcoxon Signed Ranks Test was used, and *p* values <.05 were considered significant. Statistical analyses were done with GraphPad Prism version 5.00 for Windows.

RESULTS

Characterization of MSC, CD34⁺ Cells, and MSC-EV

In all the assays, MSCs were characterized according to the definition criteria established by ISCT [29] and as previously described [27] (Supporting Information Fig. S1). The viability of MSC at the time when EV were collected was over 77% in all cases.

CD34⁺ progenitor cell purity after immunomagnetic sorting was in all cases >85%. The viability was higher than 80% in all cases.

EV size evaluated by NTA was homogeneous among samples with a mean of 131.93 nm (range: 124.4–143.6 nm). Mean particle concentration was 9.09×10^{10} particles per milliliter (range: 5.16×10^{10} – 1.21×10^{11} ; Fig. 1A). In addition, the characteristic rounded morphology of EV with a hypodense center and the typical bilayer membrane was observed by TEM. (Fig. 1B) Next, FC analysis showed that all EV had a size smaller than 1 μ m, were negative for hematopoietic markers as CD34 and CD45, and positive for MSC markers (as CD90 and CD44) and exosome markers (as CD81 and CD63). Unstained EV were used as control. (Fig. 1C) Finally, by Western blot analysis, the characteristic expression of CD63 was also demonstrated (Fig. 1D). These results fulfill the recommendations of the International Society of Extracellular Vesicles [38].

Incorporation of MSC-EV into CD34⁺ Cells

The incorporation was first demonstrated by FC, and as it is shown in (Fig. 2A), the median of cells that had incorporated EV after 24 hours of coinubation was 40.34%. As a control, culture media without EV was labeled with Vybrant Dil and incubated in the same conditions with CD34⁺ cells. The incorporation was negative as well as when CD34⁺ cells were cultured alone for 24 hours.

To confirm these results, incorporation of MSC-EV into CD34⁺ cells was also demonstrated by confocal microscopy (Fig. 2B).

In addition, the reverse transcription polymerase chain reaction expression of *SDF-1* and *COL1A1*, genes that are described to be highly expressed in MSC, was increased in CD34⁺ cells that had been incubated with EV compared with control CD34⁺ cells (Fig. 2C).

Gene Expression Profiling of CD34⁺ Cells

In order to obtain a global view of the changes induced on CD34⁺ cells after the incorporation of MSC-EV, the gene expression profiling (GEP) of five samples was analyzed.

Applying SAM analysis, we found statistically significant differences in the expression of 608 genes between CD34⁺ cells alone and CD34⁺ cells that had incorporated MSC-EV out of 7,460 tested genes by applying the established filtering criteria.

Of them, 176 genes were upregulated and 432 genes were downregulated after the incorporation. These genes were involved in several pathways. One of these pathways was apoptosis where 12 genes were altered, among which some proapoptotic genes as *CASP3* and *CASP6* were downregulated, whereas some anti-apoptotic genes as *BIRC2*, *BIRC3*, and *NFKB* were upregulated. Another altered pathway was Janus kinase (JAK)-STAT that, overall, was upregulated. Hematopoietic cell lineage pathway had also some upregulated genes as *IL11*, *CD22*, and *IL3RA* involved in hematopoietic colony formation. Also cytokine-cytokine receptor interaction pathway was upregulated (Fig. 3; Supporting Information Table S1). Also, CD44, very important molecule in hematopoietic engraftment, and prostaglandin-endoperoxide synthase 1 (*PTGS1*, *COX1*), precursor of prostaglandine E2 (*PGE₂*), were upregulated within the incorporation of MSC-EV.

Incorporation of MSC-EV into CD34⁺ Cells Increases Their Viability and Decreases Their Caspase Activity

As we observed in the GEP analysis, the incorporation of MSC-EV into CD34⁺ cells could induce changes in the genes involved in viability/apoptosis. In order to confirm these results, cell viability assay was performed after 24 hours (*n* = 14) and 48 hours (*n* = 11) of coculture with EV. After 24 hours of culture, 87.01% (80.19%–93.02%) of CD34⁺ cells were viable, and the incorporation of EV did not show any benefit in terms of early viability. However, after 48 hours of culture, CD34⁺ cells which incorporated MSC-EV had a significantly higher median viability compared with control cells, 72.19% (range: 67.85%–83.7%) versus 67.28% (range 63.66%–72.62%). This increase in cell viability was related to a significant decrease of late apoptotic cells (Annexin V⁺/7-AAD⁺) and dead cells (Annexin V⁻/7-AAD⁺; Fig. 4A). Besides, caspase 3/7 and caspase 9 activity was measured after 24 of coculture (*n* = 10). We observed a significant decrease in the activity of both caspase 3/7 and caspase 9 after the incorporation of MSC-EV in CD34⁺ cells (Fig. 4B).

Incorporation of MSC-EV into CD34⁺ Cells Do Not Significantly Modifies Cell Cycle S-Phase

To further investigate the implication of EV incorporation into CD34⁺ cells, cell cycle was studied in 11 samples. Cell cycle results showed that after 24 hours of culture, the percentage of cells in S phase was similar in the MSC-EV group (1.725 ± 0.3) compared with CD34⁺ controls (1.501 ± 0.22). However, we detected a significant decrease in the percentage of cells in phase G₀/G₁ in CD34⁺ cells that have incorporated MSC-EV (*p* = .032; Fig. 4C).

Expression of Genes Involved in Hematopoiesis in CD34⁺ Cells

Protein expression of genes involved in the maintenance of hematopoiesis was studied by FC. We detected a significant increase of CD44 expression after the incorporation of MSC-EV into CD34⁺ cells (already shown in the GEP analysis). We did not find significant changes in C-X-C chemokine receptor type 4 (*CXCR4*), Integrin Subunit Alpha 4 (*ITGA-4*), and c-KIT expression (Fig. 5A).

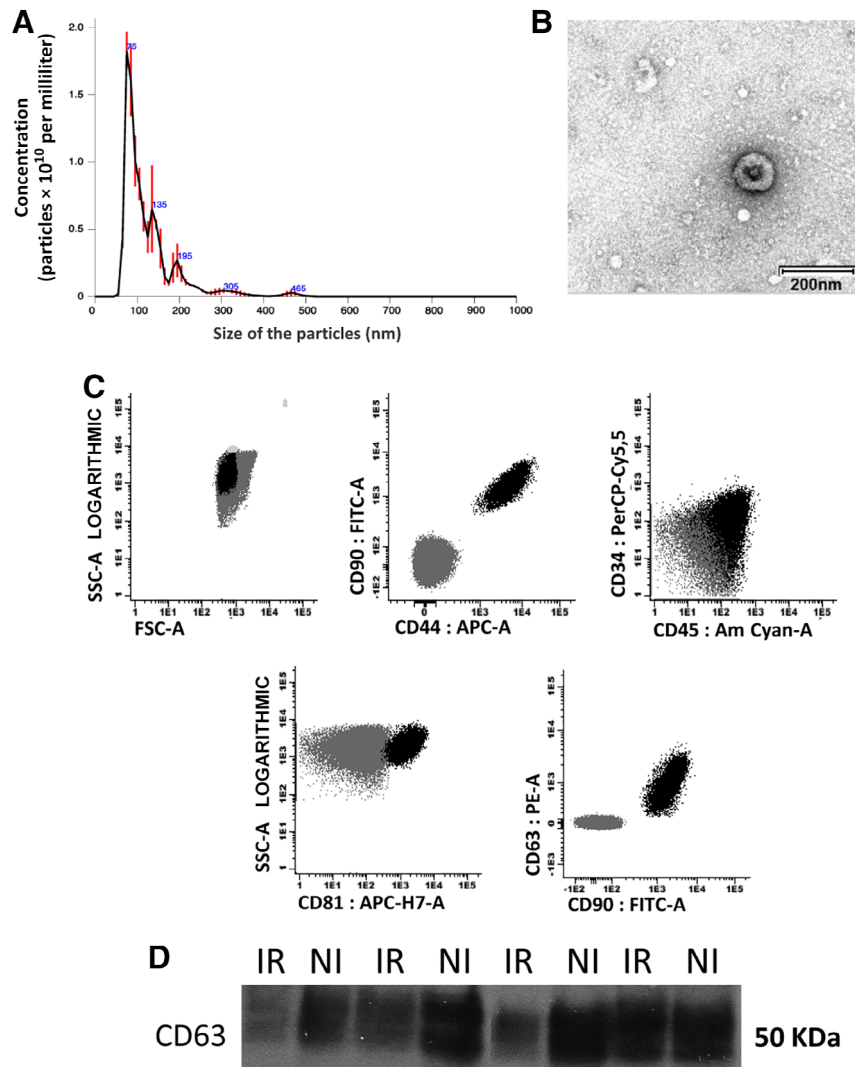


Figure 1. Characterization of extracellular vesicles (EV) released from mesenchymal stromal cells (MSC). Size distribution (nm) and concentration (particles $\times 10^{10}$ per milliliter) quantified by nanoparticle tracking analysis. **(A):** Representative graph for one sample of EV obtained from 3×10^6 MSC. **(B):** EV samples contrasted with uranyl-oxalate solution and examined under a transmission electron microscope. Scale bar = 200 nm, original magnification $\times 8,000$. Representative image of flow cytometry characterization of EV in one sample. Gates of EV were defined in the forward and side scatter dot plot by setting the upper size limit in 1 μ m. Microbeads with a diameter of 1 μ m were used for that purpose. The other dot plots represent EV stained with hematopoietic markers (CD34 and CD45), mesenchymal markers (CD90 and CD44), and exosomes markers (CD81 and CD63). Unstained controls are shown in gray, and EV stained with different antibodies are represented in black. **(C):** Samples were acquired on a FACS Calibur flow cytometer. **(D):** EV characterization by Western blot assay for the expression of CD63. Abbreviations: SSC, side scatter; FSC, forward scatter.

By WES Simple, we have also detected an increase in the levels of phospho-STAT5 after the incorporation of MSC-EV in CD34⁺ cells. The ratio phospho-STAT5/STAT5 increases in all cases after the incorporation of MSC-EV but the increase is heterogeneous among different samples of MSC-EV (Fig. 5B). These results were confirmed by FC where an increase in the mean of fluorescence intensity of p-STAT5 after the incorporation of MSC-EV in CD34⁺ cells was observed (Supporting Information Fig. S5).

Incorporation of MSC-EV into CD34⁺ Cells Increases Their Clonogenic Capacity

Clonogenic studies were performed in 10 samples. We observed that the capacity of CD34⁺ to form CFU-GM was significantly higher in those cells that had incorporated MSC-EV compared

with control CD34⁺ cells ($p = .032$). There were no differences in the size or shape of colonies between both experimental groups (Fig. 5C). The same results were observed in a subset of experiments performed with cord-blood CD34⁺ cells (Supporting Information Fig. S2).

Incorporation of MSC-EV into CD34⁺ Cells Increases Their BM Lodging Ability in NOD/SCID Mice

In vivo effects of the incorporation of MSC-EV were analyzed in a hematopoietic xenotransplantation model. For that, CD34⁺ cells with or without EV incorporation were injected intrafemorally into NOD/SCID mice. Human chimerism (human CD45⁺ cell percentage) after 4 weeks was analyzed in both the injected (right) and noninjected (left) femurs and the spleen ($n = 10$; Fig. 6).

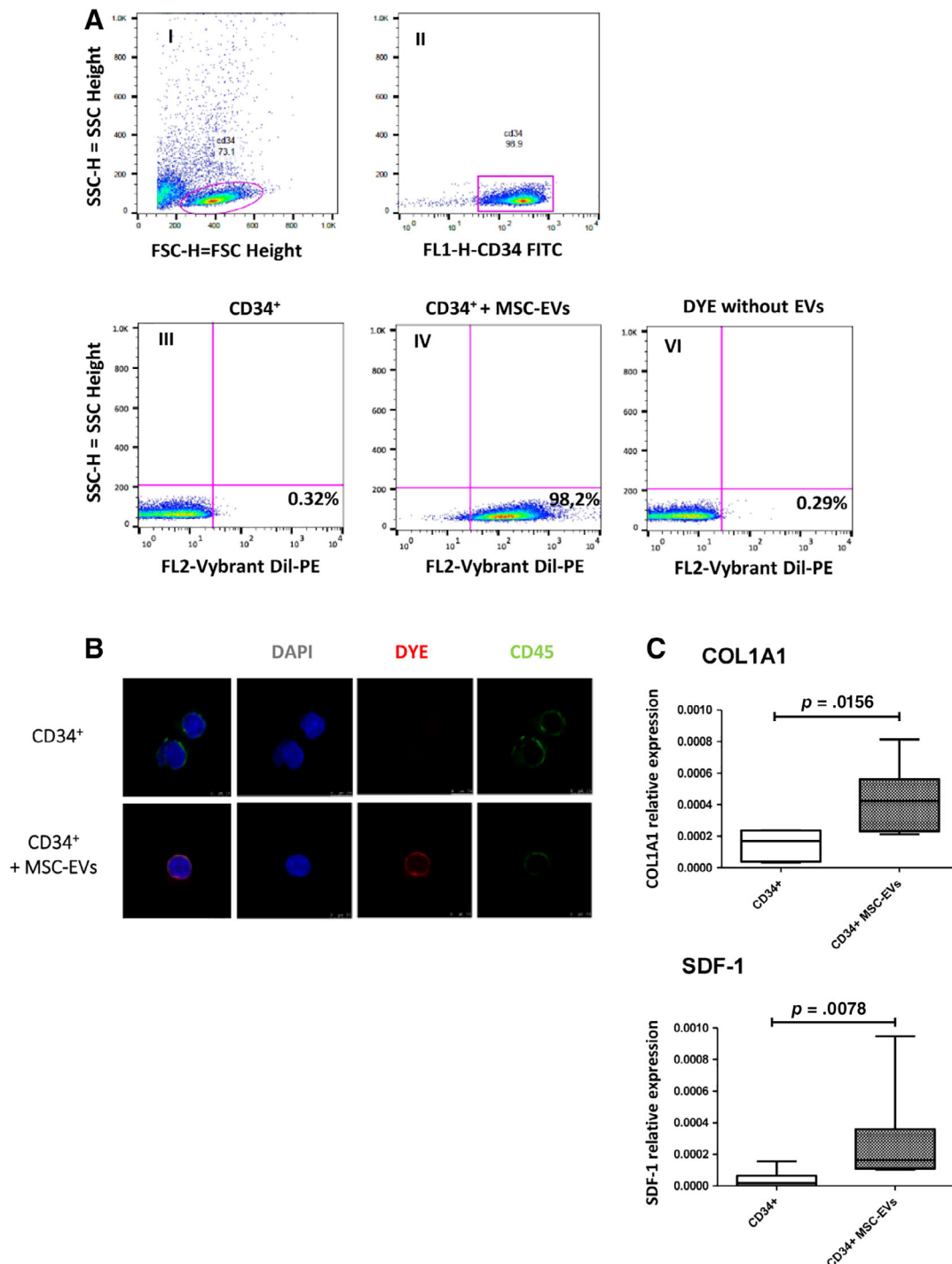


Figure 2. Uptake of EV from MSC into CD34⁺ cells. EV previously stained with fluorescent dye Vybrant Dil cell labeling solution (red) were cultured with CD34⁺ cells for 24 hours. Representative images of the incorporation after 24 hours by flow cytometry in one sample. The first two dot plots show the forward and side scatter axes (I) and the gate of cells that are positive for CD34 Ab (II). The other dot plots represent the percentage of CD34⁺ cells that have incorporated EV: CD34⁺ cells alone (III), CD34⁺ cells cultured with MSC-EV (IV), and CD34⁺ cells cultured with supernatant without EV, stained with Vybrant Dil (V). (A): Samples were acquired on a FACS Calibur flow cytometer. Representative images of the incorporation after 24 hours by confocal microscopy in one sample. Scale bar = 7.5 μ m. CD34⁺ cells were labeled with anti-CD45 ab (in green). Nuclei were stained with DAPI (blue). (B): Images in the top row represent cells without EV; images in the bottom row are from CD34⁺ cells that had incorporated MSC-EV. Relative expression of SDF-1 and COL1A1 in CD34⁺ alone or cultured with MSC-EV performed by reverse transcription polymerase chain reaction. (C): Glyceraldehyde-3-phosphate dehydrogenase was used as control $n = 10$. Abbreviations: COL1A1, collagen type i alpha 1; DAPI: 4',6-diamidino-2-phenylindole; EV, extracellular vesicles; FSC, forward scatter; MSC, mesenchymal stromal cells; SDF-1, stromal-cell-derived factor-1; SSC, side scatter.

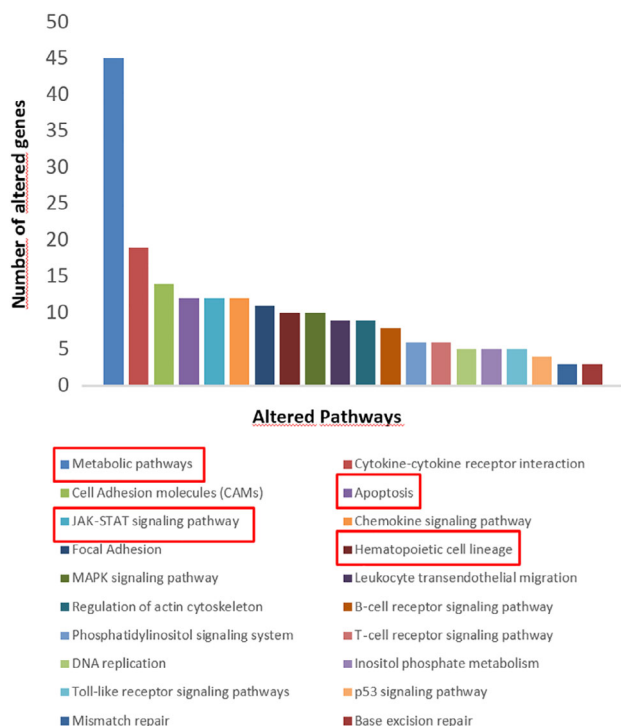


Figure 3. Gene expression profiling of CD34⁺ cells. Purified RNA from five samples in both conditions (alone or with mesenchymal stromal cells-extracellular vesicles) was hybridized in gene expression arrays (Affymetrix). The significance analysis of microarrays technique was used for the identification of differentially expressed genes among samples. Column graph representing the most altered pathways after a pathway analysis using the KEGG [Kyoto Encyclopedia of Genes and Genomes] database and Webgestalt.

The percentage of human CD45⁺ cells in the injected femur was significantly higher in mice transplanted with CD34⁺ that had incorporated MSC-EV ($p = .027$) compared with CD34⁺ cells alone (Fig. 6A). Nevertheless, we did not observe significant differences between both groups in the left femurs and spleens (Fig. 6A).

In order to analyze multilineage cell engraftment, cell subpopulations were evaluated only in the injected femurs (right) due to their higher engraftment. We found higher levels of human CD34⁺, CD14⁺, CD13⁺, and CD19⁺ cells in mice transplanted with CD34⁺ cells that had incorporated MSC-EV compared with CD34⁺ cells alone, but these differences were not significant (Fig. 6B).

DISCUSSION

The current work validates the potential role of a new approach to benefit from the effects of MSC administration on hematopoietic function of CD34⁺ cells in the transplant setting: preincubating human CD34⁺ cells with EV derived from human MSC and infusing only the CD34⁺ cells. This strategy significantly increases the in vitro clonogenic ability of CD34⁺ cells but most importantly increase their 4-week BM lodging ability in vivo in the injected femur.

There is extensive information on the role of MSC to improve the hematopoietic engraftment [9, 39–42], and the administration of MSC to improve engraftment is being explored in clinical trials. As MSC may exert some of their effects through the

release of EV [24, 43, 44], there are some preclinical studies that have explored the role of MSC-EV in the improvement of hematopoiesis after hematopoietic transplantation [25, 45, 46] and to analyze the MSC-EV influence on CD34⁺ cells gene expression pattern, altering their survival and promoting their homing to the BM [26]. In this regard, we have observed that the incorporation of MSC-EV into CD34⁺ cells modifies the expression of some genes (176 upregulated and 432 downregulated) compared with control CD34⁺ cells. Some of these genes were involved in apoptosis. Therefore, we confirmed by FC that apoptosis was significantly decreased in CD34⁺ cells that incorporated vesicles. This is in accordance with findings that MSC-EV can down-regulate phosphorylation of H2AX after damage to CD34⁺ cells, leading to a better DNA repair efficiency and the inhibition of apoptosis [47]. It has also been reported that the mechanisms underlying recovery of CD34⁺ cells by MSC-EV are not only due to a decrease in apoptosis but also due to a stimulation of proliferation. We have observed an upregulation of JAK-STAT pathway and confirmed the increased levels of STAT5 phosphorylation by WES Simple and FC after the incorporation of MSC-EV in CD34⁺ cells. Although there are no previous data on the implications of this (probably transient) upregulation of JAK-STAT on CD34⁺ cells induced by MSC-EV incorporation, it is well established that a constitutive upregulation of this signaling pathway (as observed in V617F JAK-2 mutations in myeloproliferative neoplasms) leads to CD34⁺ cell proliferation and reduced apoptosis [48, 49]. In addition, an upregulation of JAK/STAT signaling has been shown in CD34⁺ cells from acute myeloid leukemia patients compared with normal cord blood or peripheral blood stem cells, suggesting that JAK/STAT signaling supports AML cells growth and survival [50, 51]. In addition, De Luca et al. demonstrated that MSC-EV miRNAs and piRNAs influence CD34⁺ cells gene profile, inducing cell survival and proliferation in all the hematopoietic lineages [26].

We have also shown that MSC-EV carry bioactive molecules and can transfer mRNA and proteins to the target cells [23, 34]. The bioactive cargo enclosed in MSC-EV may play a role in favoring hematopoietic engraftment. In fact, we have shown that the expression of CD44, a well-known factor involved in cell adhesion and migration, is increased after the incorporation of MSC-EV into CD34⁺ cells. These results are consistent with findings that MSC-EV carry mRNA for CD44 [52], we also have confirmed that MSC-EV express CD44 protein on their surface. The effects may not involve CXCR4, another important factor for homing and engraftment, as we have not observed changes in its expression after the incorporation of MSC-EV, although some groups have described an increase in its expression [26]. This discordance may be related to different experimental conditions (e.g., the latter results were obtained in cord-blood CD34⁺ cells, whereas our in vitro experiments were performed with G-CSF mobilized adult CD34⁺ cells). In this regard, we performed some of the experiments with cord blood cells (Supporting Information Fig. S2), and with cord blood cells, the increase in CXCR4 expression after MSC-EV incorporation is significantly increased. In addition, the fact that we have observed that CD34⁺ cells gain SDF-1 expression after the incorporation of MSC-EV warrants a specific comment. The importance of the SDF-1/CXCR4 axis in CD34⁺ cells homing and engraftment is unquestionable but is generally considered only in the most important direction, which is the interaction between SDF-1 expressed in MSC and CXCR4 expressed in CD34⁺ cells. However, MSC can also express low levels of CXCR4

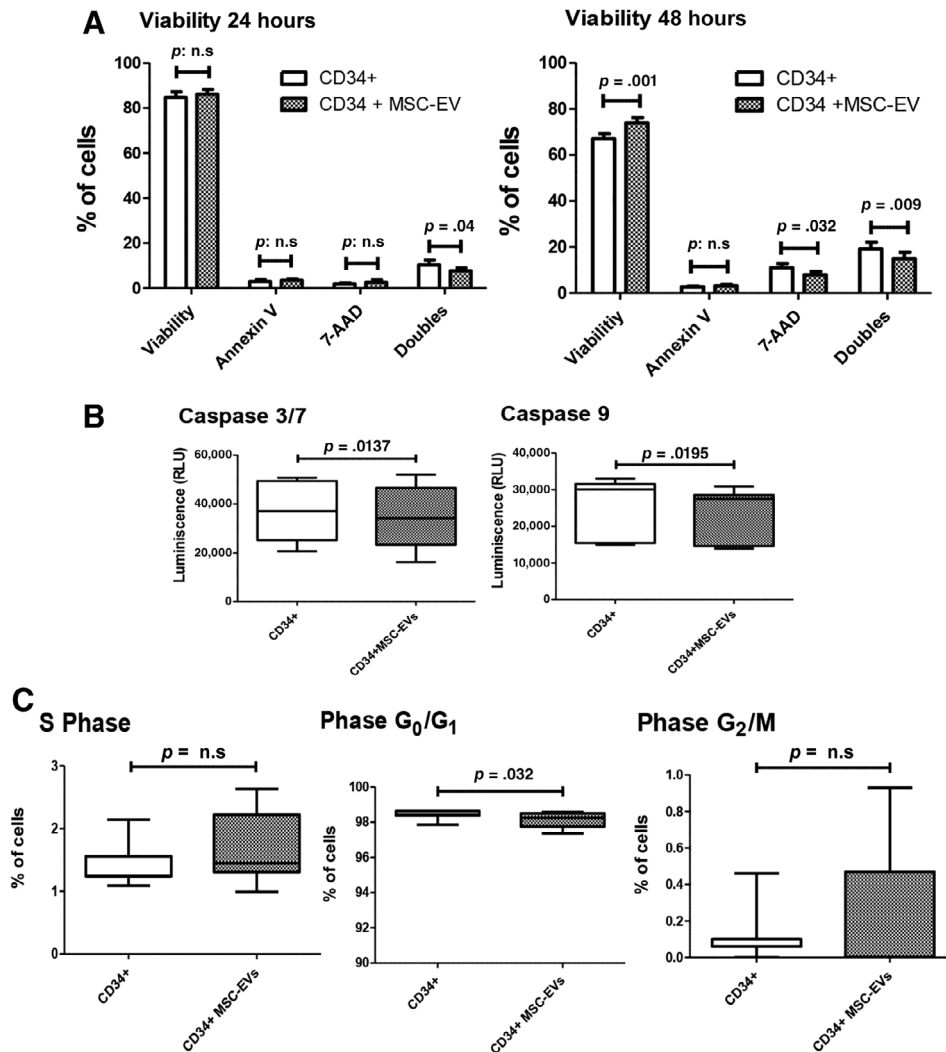


Figure 4. Viability, caspase activity, and proliferation of CD34⁺ cells. Apoptosis assays in CD34⁺ cells alone or CD34⁺ cells that have incorporated MSC-EV after 24 and 48 hours of culture. CD34⁺ cells were incubated with Annexin V, 7-AAD, and CD34, and the expression of different cell surface markers was analyzed by flow cytometry. Cells were considered to be viable (Annexin V⁻/7-AAD⁻), in an early apoptotic state (Annexin V⁺/7-AAD⁻), late apoptosis (Annexin V⁺/7-AAD⁺), or dead (Annexin V⁻/7-AAD⁺). **(A):** Data expressed as mean of the percentage of cells in the different conditions, caspase activity assays in CD34⁺ cells alone or CD34⁺ cells that have incorporated MSC-EV after 24 hours of culture. **(B):** Luminiscence is expressed as the number of relRLU. Cell cycle profiling of CD34⁺ cells after 24 hours of incubation with MSC-EV analyzed by flow cytometry. **(C):** Data are represented as mean of the percentage of cells in each phase. Ten experiments were done for each group. Abbreviations: 7-AAD, 7-amino-actinomycin; EV, extracellular vesicles; MSC, mesenchymal stromal cells; RLU, relative light unit.

[53–55], so the fact that CD34⁺ cells express SDF-1 could also potentially favors the interaction between SDF-1 and CXCR4, enhancing the engraftment ability of CD34⁺ cells. We have also found an increased expression of PTGS1, precursor of PGE₂ after the incorporation of MSC-EV. PGE₂ enhances CD34⁺ cells homing, survival, and proliferation [56].

Besides these changes in gene and protein expression after the incorporation of MSC-EV into CD34⁺ cells, the most important questions are related to the potential functional implications of these changes. As it has been mentioned, we have addressed them both in vitro and in vivo. Interestingly, the in vitro clonogenic assays revealed a significant increase in colony formation after MSC-EV incorporation. This is again in agreement with the upregulation of some molecules involved in hematopoiesis as IL11, CD22, and IL3RA that were shown

in the GEP analysis. Other reports support these findings showing higher colony outgrowth after treatment of CD34⁺ cells with MSC-EV [25, 45, 47].

The latest and most relevant test was to evaluate whether MSC-EV could improve in vivo engraftment of CD34⁺ cells. For this experiments, we used cord blood CD34⁺ cells, as their engraftment capacity is higher, in order to reduce the number of cells and vesicles needed for each experiment [57] but maintaining the proportion of MSC-EV/ CD34⁺ cells we have previously used in all the in vitro experiments. We have observed a significant better BM lodging ability in the injected femurs after 4 weeks in mice with human CD34⁺ cells that had incorporated human MSC-EV in comparison with the lodging of control CD34⁺ cells. In accordance with our results, De Luca et al. analyzed the homing into the BM of intravenously

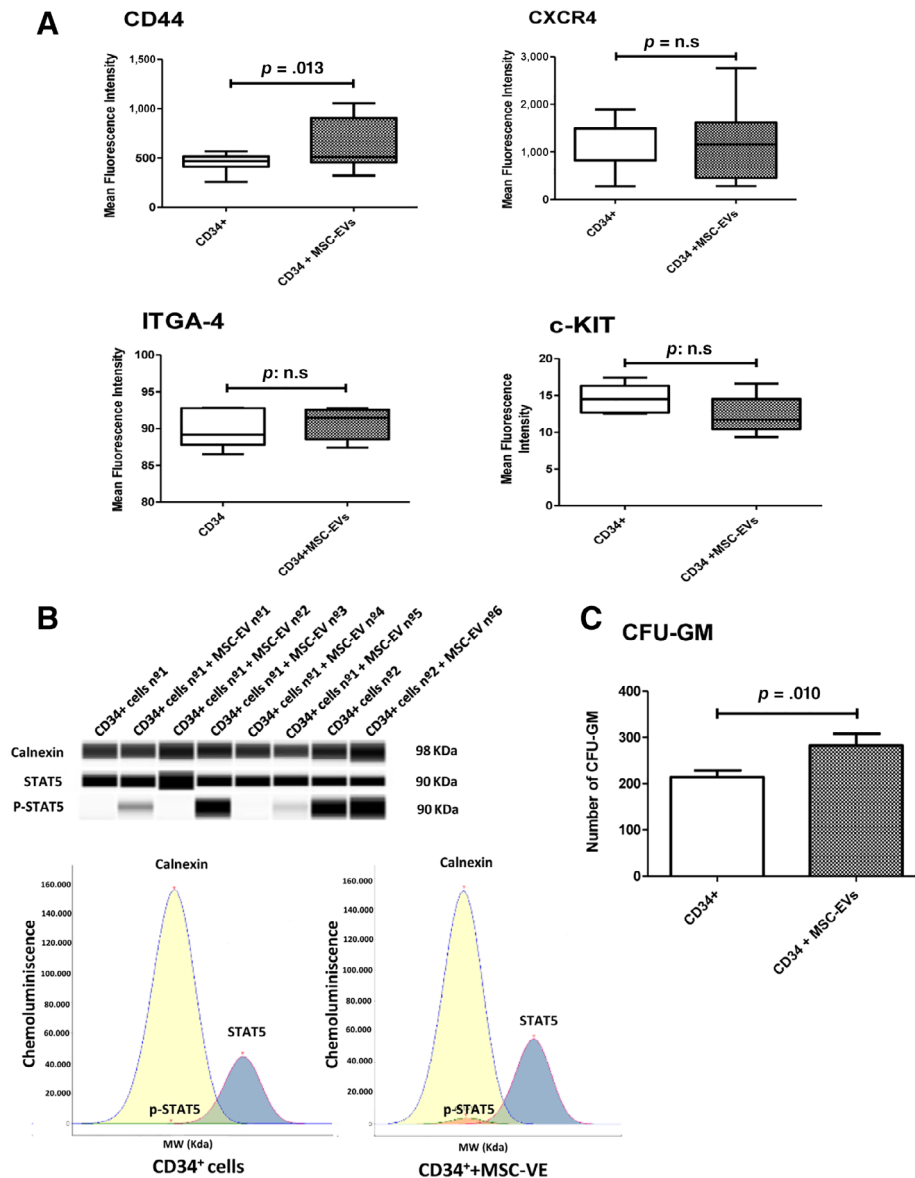


Figure 5. Expression of proteins involved in hematopoiesis on CD34⁺ cells and their capacity of colony formation. Mean fluorescence intensity of different proteins involved in hematopoiesis maintenance as CD44, CXCR4, ITGA-4, and c-KIT was evaluated by FACS analysis. **(A):** Samples were acquired on a FACS Calibur flow cytometer. **(B):** Results from Calnexin, STAT5, and phospho-STAT5 quantification in CD34⁺ cells, visualized as virtual blots (up) or peaks (only one representative sample of CD34⁺ cells and other representative sample of CD34⁺ cells that have incorporated MSC-EV) (down), analyzed by WES Simple technology using Compass software. Total CFU-GM from CD34⁺ cells were scored after 14 days in methylcellulose medium. **(C):** CD34⁺ cells were cultured with or without EV for 24 hours and then, 1,500 cells were seeded into methylcellulose medium. Data are represented as mean of 10 experiments for each group. Abbreviations: CFU-GM, colony-forming unit granulocyte/macrophage; EV, extracellular vesicles; MSC, mesenchymal stromal cells.

(instead of intravenously) administered human CD34⁺ cells with incorporated vesicles only 24 hours after the injection [26], but human engraftment at later time points was not studied in their work. Other authors have found potential beneficial effects of either murine or human MSC-EV in different results with different experimental designs different from our approach. In this regard, Wen et al. showed that murine or human MSC-EV improves the engraftment of murine CD34⁺ cells damaged by irradiation [47], and Schoefinius et al. found that the injection of MSC-EV rescues hematopoiesis in irradiated mice without the addition of CD34⁺ cells [25]. We have not found differences in the percentage of human cells neither in the contralateral femur nor in the spleen of these mice.

Regarding these results, several groups have described that intrabone transplantation results in higher human cell engraftment or chimerism in the injected femurs, whereas engraftment at distal hematopoietic sites as the peripheral blood, spleen, and contralateral femur could be lower. Some studies suggest that the retention of human cells in the BM after intrabone injection enhances local chimerism at expense of systemic chimerism [58,59]. Furthermore, prior published studies from our own group also showed higher engraftment in the injected femur when compared with the contralateral femur [9]. It could be hypothesized that MSC-EV incorporation into CD34⁺ cells may only improve lodging and retention in the injected femur but not in the homing ability or that the

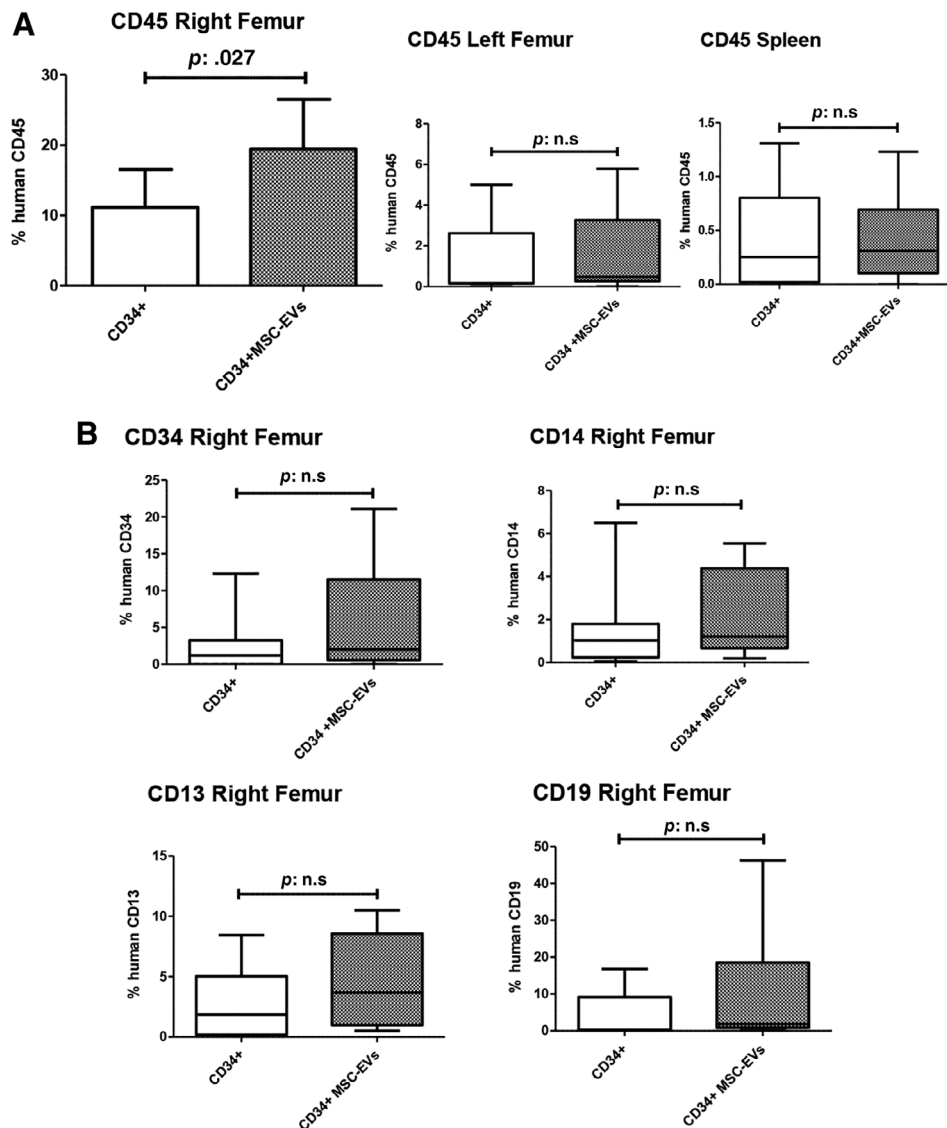


Figure 6. Analysis of human hematopoietic lodging in nonobese diabetic/severe combined immunodeficient mice. The percentage of human CD45⁺ cells (donor chimerism) in total bone marrow samples from both the femurs, right (injected site) (A) and left (contralateral) (B), and spleen (C) at 4 weeks after hematopoietic transplantation was analyzed by flow cytometry. Percentage of human hematopoietic subpopulations (CD34, CD14, CD13, and CD19) in right femur bone marrow at week 4 (D). Data are represented as mean of 10 experiments for each group. Abbreviations: EV, extracellular vesicles; MSC, mesenchymal stromal cells.

increase in engraftment in the injected femur is not enough to compensate that of other distal BM niches.

CONCLUSION

In this study, we have demonstrated that human MSC-EV are able to incorporate into human CD34⁺ cells, modifying their gene expression and increasing their viability, clonogenic capacity in vitro, and their 4-week BM lodging ability in vivo in the injected femurs in a xenotransplantation model.

ACKNOWLEDGMENTS

This work was partially supported by Fondo de Investigaciones Sanitarias, Instituto de Salud Carlos III (Grants PI12/01775 and PI16/01407), Consejería de Educación (Grants HUS308U14 and

CAS079P17), and Consejería de Sanidad de Castilla y León (Grants GRS1348/A/19 and GRS1621/A/17), Junta de Castilla y León. S.P. is supported by Santander-USAL grant, N.E.-L. is supported by FEHH, L.O. is supported by Consejería de Educación, JCYL, A.R. is supported by IBSAL, and S.M. is supported by ISCIII.

AUTHOR CONTRIBUTIONS

C.d.C.: conception/design, data interpretation, reviewed the manuscript, final approval of manuscript; F.S.-G.: conception/design, data interpretation, manuscript writing, reviewed the manuscript, final approval of manuscript; S.P.: collection and/or assembly of data, sample preparation, most experiments and statistical analysis, murine experiments, manuscript writing, reviewed the manuscript, final approval of manuscript; S.M.:

collection and/or assembly of data, performed sample preparation, most experiments and statistical analysis, manuscript writing, reviewed the manuscript, final approval of manuscript; L.O. and T.L.R.: performed and analyzed flow cytometry studies, reviewed the manuscript, final approval of manuscript; L.A.C.: performed overall bioinformatics analysis, reviewed the manuscript, final approval of manuscript; M.D.-C.: provision of study patients, reviewed the manuscript, final approval of manuscript; A.R.: collaborate with confocal microscopy experiments, reviewed the manuscript, final approval of manuscript; N.E.-L.: help with

reverse transcription polymerase chain reaction studies, reviewed the manuscript, final approval of manuscript; A.G.d.I.T.: performed experiments with mice, reviewed the manuscript, final approval of manuscript; I.G.: provision of cord blood samples, reviewed the manuscript, final approval of manuscript.

DISCLOSURE OF POTENTIAL CONFLICTS OF INTEREST

The authors indicated no potential conflicts of interest.

REFERENCES

- Gyurkocza B, Rezvani A, Storb RF. Allogeneic hematopoietic cell transplantation: The state of the art. *Expert Rev Hematol* 2010;3:285–299.
- Roncarolo MG, Gregori S, Lucarelli B et al. Clinical tolerance in allogeneic hematopoietic stem cell transplantation. *Immunol Rev* 2011;241:145–163.
- Szyska M, Na IK. Bone marrow GvHD after allogeneic hematopoietic stem cell transplantation. *Front Immunol* 2016;7:118.
- Rieger K, Marinets O, Fietz T et al. Mesenchymal stem cells remain of host origin even a long time after allogeneic peripheral blood stem cell or bone marrow transplantation. *Exp Hematol* 2005;33:605–611.
- Wang Y, Zhu G, Wang J et al. Irradiation alters the differentiation potential of bone marrow mesenchymal stem cells. *Mol Med Res* 2016;13:213–223.
- Minguell JJ, Conget P, Erices A. Biology and clinical utilization of mesenchymal progenitor cells. *Braz J Med Biol Res* 2000;33:881–887.
- Fernandez-Garcia M, Yanez RM, Sanchez-Dominguez R et al. Mesenchymal stromal cells enhance the engraftment of hematopoietic stem cells in an autologous mouse transplantation model. *Stem Cell Res Ther* 2015;6:165.
- Carrancio S, Blanco B, Romo C et al. Bone marrow mesenchymal stem cells for improving hematopoietic function: An in vitro and in vivo model. Part 2: Effect on bone marrow microenvironment. *PLoS One* 2011;6:e26241.
- Carrancio S, Romo C, Ramos T et al. Effects of MSC coadministration and route of delivery on cord blood hematopoietic stem cell engraftment. *Cell Transplant* 2013;22:1171–1183.
- Hiwase SD, Dyson PG, To LB et al. Cotransplantation of placental mesenchymal stromal cells enhances single and double cord blood engraftment in nonobese diabetic/severe combined immune deficient mice. *STEM CELLS* 2009;27:2293–2300.
- Yang X, Balakrishnan I, Torok-Storb B et al. Marrow stromal cell infusion rescues hematopoiesis in lethally irradiated mice despite rapid clearance after infusion. *Adv Hematol* 2012;2012:142530.
- Angelopoulou M, Novelli E, Grove JE et al. Cotransplantation of human mesenchymal stem cells enhances human myelopoiesis and megakaryocytopoiesis in NOD/SCID mice. *Exp Hematol* 2003;31:413–420.
- Mohammadali F, Abroun S, Atashi A. Mild hypoxia and human bone marrow mesenchymal stem cells synergistically enhance expansion and homing capacity of human cord blood CD34+ stem cells. *Iran J Basic Med Sci* 2018;21:709–716.
- Sanchez-Guijo FM, Lopez-Villar O, Lopez-Anglada L et al. Allogeneic mesenchymal stem cell therapy for refractory cytopenias after hematopoietic stem cell transplantation. *Transfusion* 2012;52:1086–1091.
- De Luca L, Trino S, Laurenzana I et al. Mesenchymal stem cell derived extracellular vesicles: A role in hematopoietic transplantation? *Int J Mol Sci* 2017;18:E1022.
- Harting MT, Srivastava AK, Zhaorigetu S et al. Inflammation-stimulated mesenchymal stromal cell-derived extracellular vesicles attenuate inflammation. *STEM CELLS* 2018;36:79–90.
- Mao F, Tu Q, Wang L et al. Mesenchymal stem cells and their therapeutic applications in inflammatory bowel disease. *Oncotarget* 2017;8:38008–38021.
- Tkach M, Thery C. Communication by extracellular vesicles: Where we are and where we need to go. *Cell* 2016;164:1226–1232.
- Zaborowski MP, Balaj L, Breakefield XO et al. Extracellular vesicles: Composition, biological relevance, and methods of study. *BioScience* 2015;65:783–797.
- Yuana Y, Sturk A, Nieuwland R. Extracellular vesicles in physiological and pathological conditions. *Blood Rev* 2013;27:31–39.
- Collino F, Deregibus MC, Bruno S et al. Microvesicles derived from adult human bone marrow and tissue specific mesenchymal stem cells shuttle selected pattern of miRNAs. *PLoS One* 2010;5:e11803.
- Raposo G, Stoorvogel W. Extracellular vesicles: Exosomes, microvesicles, and friends. *J Cell Biol* 2013;200:373–383.
- Muntion S, Ramos TL, Diez-Campelo M et al. Microvesicles from mesenchymal stromal cells are involved in HPC-microenvironment crosstalk in myelodysplastic patients. *PLoS One* 2016;11:e0146722.
- Gatti S, Bruno S, Deregibus MC et al. Microvesicles derived from human adult mesenchymal stem cells protect against ischaemia-reperfusion-induced acute and chronic kidney injury. *Nephrol Dial Transplant* 2011;26:1474–1483.
- Schoefinius JS, Brunswig-Spickenheier B, Speiseder T et al. Mesenchymal stromal cell-derived extracellular vesicles provide long-term survival after total body irradiation without additional hematopoietic stem cell support. *STEM CELLS* 2017;35:2379–2389.
- De Luca L, Trino S, Laurenzana I et al. MiRNAs and piRNAs from bone marrow mesenchymal stem cell extracellular vesicles induce cell survival and inhibit cell differentiation of cord blood hematopoietic stem cells: A new insight in transplantation. *Oncotarget* 2016;7:6676–6692.
- Preciado S, Muntion S, Rico A et al. Mesenchymal stromal cell irradiation interferes with the adipogenic/osteogenic differentiation balance and improves their hematopoietic-supporting ability. *Biol Blood Marrow Transplant* 2018;24:443–451.
- Carrancio S, Lopez-Holgado N, Sanchez-Guijo FM et al. Optimization of mesenchymal stem cell expansion procedures by cell separation and culture conditions modification. *Exp Hematol* 2008;36:1014–1021.
- Dominici M, Le Blanc K, Mueller I et al. Minimal criteria for defining multipotent mesenchymal stromal cells. The International Society for Cellular Therapy position statement. *Cytotherapy* 2006;8:315–317.
- Ramirez M, Regidor C, Marugan I et al. Engraftment kinetics of human CD34+ cells from cord blood and mobilized peripheral blood co-transplanted into NOD/SCID mice. *Bone Marrow Transplant* 2005;35:271–275.
- Thery C, Amigorena S, Raposo G et al. Isolation and characterization of exosomes from cell culture supernatants and biological fluids. *Curr Protoc Cell Biol* 2006;3.22.1–3.22.29; Chapter 3(Unit 3.22).
- van der Pol E, Coumans FA, Grootemaat AE et al. Particle size distribution of exosomes and microvesicles determined by transmission electron microscopy, flow cytometry, nanoparticle tracking analysis, and resistive pulse sensing. *J Thromb Haemost* 2014;12:1182–1192.
- T LR, Sanchez-Abarca LI, Muntion S et al. MSC surface markers (CD44, CD73, and CD90) can identify human MSC-derived extracellular vesicles by conventional flow cytometry. *Cell Commun Signal* 2016;14:1.
- Ramos TL, Sanchez-Abarca LI, Lopez-Ruano G et al. Do endothelial cells belong to the primitive stem leukemic clone in CML? Role of extracellular vesicles. *Leuk Res* 2015;39:921–924.
- Wang J, Vasaikar S, Shi Z et al. WebGestalt 2017: A more comprehensive, powerful, flexible and interactive gene set enrichment analysis toolkit. *Nucleic Acids Res* 2017;45:W130–W137.
- Misiewicz-Krzeminska I, Corchete IA, Rojas EA et al. A novel nano-immunoassay method for quantification of proteins from CD138-purified myeloma cells: Biological and clinical utility. *Haematologica* 2018;103:880–889.

- 37** Verlinden SF, van Es HH, van Bekkum DW. Serial bone marrow sampling for long-term follow up of human hematopoiesis in NOD/SCID mice. *Exp Hematol* 1998;26:627–630.
- 38** Lotvall J, Hill AF, Hochberg F et al. Minimal experimental requirements for definition of extracellular vesicles and their functions: A position statement from the International Society for Extracellular Vesicles. *J Extracellular Vesicles* 2014;3:26913.
- 39** Ball LM, Bernardo ME, Roelofs H et al. Cotransplantation of ex vivo expanded mesenchymal stem cells accelerates lymphocyte recovery and may reduce the risk of graft failure in haploidentical hematopoietic stem-cell transplantation. *Blood* 2007;110:2764–2767.
- 40** Bernardo ME, Fibbe WE. Mesenchymal stromal cells and hematopoietic stem cell transplantation. *Immunol Lett* 2015;168:215–221.
- 41** Goto T, Murata M, Terakura S et al. Phase I study of cord blood transplantation with intrabone marrow injection of mesenchymal stem cells: A clinical study protocol. *Medicine* 2018;97:e0449.
- 42** Le Blanc K, Samuelsson H, Gustafsson B et al. Transplantation of mesenchymal stem cells to enhance engraftment of hematopoietic stem cells. *Leukemia* 2007;21:1733–1738.
- 43** Zhang Y, Chopp M, Meng Y et al. Effect of exosomes derived from multipotent mesenchymal stromal cells on functional recovery and neurovascular plasticity in rats after traumatic brain injury. *J Neurosurg* 2015;122:856–867.
- 44** Lai RC, Arslan F, Lee MM et al. Exosome secreted by MSC reduces myocardial ischemia/reperfusion injury. *Stem Cell Res* 2010;4:214–222.
- 45** Xie H, Sun L, Zhang L et al. Mesenchymal stem cell-derived microvesicles support ex vivo expansion of cord blood-derived CD34(+) cells. *Stem Cells Int* 2016;2016:6493241.
- 46** Timari H, Shamsasenjan K, Movassaghpour A et al. The effect of mesenchymal stem cell-derived extracellular vesicles on hematopoietic stem cells fate. *Adv Pharmaceut Bull* 2017;7:531–546.
- 47** Wen S, Dooner M, Cheng Y et al. Mesenchymal stromal cell-derived extracellular vesicles rescue radiation damage to murine marrow hematopoietic cells. *Leukemia* 2016;30:2221–2231.
- 48** Zhao R, Xing S, Li Z et al. Identification of an acquired JAK2 mutation in polycythemia vera. *J Biol Chem* 2005;280:22788–22792.
- 49** Pearson S, Williamson AJK, Blance R et al. Proteomic analysis of JAK2V617F-induced changes identifies potential new combinatorial therapeutic approaches. *Leukemia* 2017;31:2717–2725.
- 50** Cook AM, Li L, Ho Y et al. Role of altered growth factor receptor-mediated JAK2 signaling in growth and maintenance of human acute myeloid leukemia stem cells. *Blood* 2014;123:2826–2837.
- 51** Murone M, Radpour R, Attinger A et al. The multi-kinase inhibitor Debio 0617B reduces maintenance and self-renewal of primary human AML CD34(+) stem/progenitor cells. *Mol Cancer Ther* 2017;16:1497–1510.
- 52** Arasu UT, Karna R, Harkonen K et al. Human mesenchymal stem cells secrete hyaluronan-coated extracellular vesicles. *Matrix Biol* 2017;64:54–68.
- 53** Jin W, Liang X, Brooks A et al. Modelling of the SDF-1/CXCR4 regulated in vivo homing of therapeutic mesenchymal stem/stromal cells in mice. *PeerJ* 2018;6:e6072.
- 54** Ji JF, He BP, Dheen ST et al. Interactions of chemokines and chemokine receptors mediate the migration of mesenchymal stem cells to the impaired site in the brain after hypoglossal nerve injury. *STEM CELLS* 2004;22:415–427.
- 55** Jeltsch KS, Radke TF, Laufs S et al. Unrestricted somatic stem cells: Interaction with CD34+ cells in vitro and in vivo, expression of homing genes and exclusion of tumorigenic potential. *Cytotherapy* 2011;13:357–365.
- 56** Hoggatt J, Singh P, Sampath J et al. Prostaglandin E2 enhances hematopoietic stem cell homing, survival, and proliferation. *Blood* 2009;113:5444–5455.
- 57** Matsumura T, Kametani Y, Ando K et al. Functional CD5+ B cells develop predominantly in the spleen of NOD/SCID/gammac (null) (NOG) mice transplanted either with human umbilical cord blood, bone marrow, or mobilized peripheral blood CD34+ cells. *Exp Hematol* 2003;31:789–797.
- 58** Futrega K, Lott WB, Doran MR. Direct bone marrow HSC transplantation enhances local engraftment at the expense of systemic engraftment in NSG mice. *Sci Rep* 2016;6:1–17.
- 59** Yahata T, Ando K, Sato T et al. A highly sensitive strategy for SCID-repopulating cell assay by direct injection of primitive human hematopoietic cells into NOD/SCID mice bone marrow. *Blood* 2003;101:2905–2913.



See www.StemCells.com for supporting information available online.